第 29 卷第 3 期
2013 年 3 月

无 机 化 学 学 报
CHINESE JOURNAL OF INORGANIC CHEMISTRY

Vol.29 No.3
621-627

2-苯并咪唑苯基膦酸的金属有机膦酸化合物$[Mn(2\text{-}bppH_2)_2(H_2O)]_n$和$[Cu(2\text{-}bppH_2)_2]\cdot xCH_3OH$的合成、结构及性质研究

杨骁婧　鲍松松　郑丽敏*

(南京大学化学化工学院,配位化学国家重点实验室,南京　210093)

摘要：本文报道了两个 2-苯并咪唑苯基膦酸(2-bppH$_3$)的过渡金属配合物,$[Mn(2\text{-}bppH_2)_2(H_2O)]_n$ (**1**)和$[Cu(2\text{-}bppH_2)_2]\cdot xCH_3OH$ (**2**)。化合物 **1** 中 Mn 原子通过 O-P-O 桥联形成一维链状结构,而化合物 **2** 则为单核结构,单核单元之间通过氢键和 π-π 相互作用形成三维结构。在化合物 **1** 中,O-P-O 桥联的 2 个锰离子之间存在反铁磁性相互作用。

关键词：锰；铜；2-苯并咪唑苯基膦酸；单晶结构；磁性质；荧光性质

中图分类号：O614.71$^+$1；O614.121　　**文献标识码**：A　　**文章编号**：1001-4861(2012)03-0621-07

DOI:10.3969/j.issn.1001-4861.2013.00.037

Structures and Magnetic Properties of Metal Phosphonates Based on 2-(Benzoimidazol-2-yl)phenylphosphonic Acid: $[Mn(2\text{-}bppH_2)_2(H_2O)]_n$ and $[Cu(2\text{-}bppH_2)_2]\cdot xCH_3OH$

YANG Xiao-Jing　BAO Song-Song　ZHENG Li-Min*

(*State Key Laboratory of Coordination Chemistry, School of Chemistry and Chemical Engineering, Nanjing University, Nanjing* 210093, *China*)

Abstract: This paper reports two metal phosphonates $[Mn(2\text{-}bppH_2)_2(H_2O)]_n$ (**1**) and $[Cu(2\text{-}bppH_2)_2]\cdot xCH_3OH$ (**2**) based on 2-(benzoimidazol-2-yl)phenylphosphonic acid (2-bppH$_3$). Compound **1** has a one-dimensional chain structure in which Mn atoms are bridged by O-P-O units to form infinite chains. While compound **2** shows discrete mononuclear structure. Antiferromagnetic interactions are mediated between the Mn^{II} ions through the O-P-O bridge in compound **1**. CCDC: 913645, **1**; 913643, **2**.

Key words: manganese; copper; 2-(benzoimidazol-2-yl)phenylphosphonic acid; crystal structure; magnetic property; fluorescent property

0 Introduction

Increasing attention has been paid on metal phospohonate materials due to their potential applications in catalysis [1-2], nonlinear optics [3], magnetism [4-7], and biotechnology [8]. In recent years, a plenty of compounds with interesting architectures and possible functionalities have been reported by rational designing phosphonate ligands with different functional groups, such as amino [9], carboxylate [10-11], pyridyl[12-14], macrocyclic [15-16] groups etc [17]. Benzimidazole and its derivatives are important model compounds for purines because of the structural similarities [18-19]. Moreover, benzimidazole residue is a constituent of vitamin B_{12}, so the biological properties [20-22] as well as their potential use as therapeutics[23-26] have been studied extensively.

收稿日期:2012-02-16。收修改稿日期:2012-09-25。

江苏省自然科学基金 (No.BK2009009)资助项目。

*通讯联系人。E-mail:lmzheng@nju.edu.cn

Hence, the integration of benzimidazol group into metal phosphonate framework could introduce organic functional sites into the hybrid network which was constructed through weak interactions such as hydrogen-bond and π-π interactions. In the previous work of our group, a series of flexible ligands which combined the benzimidazole moiety with the phosphonate group have been used to synthesize new metal phosphonates. The reactions of bis(benzimidazol-2-ylmethyl)iminomethylenephosphonic acid (bbimpH_2, $[(C_7H_5N_2)CH_2]_2NCH_2PO_3H_2$) with different metal salts and second organic ligands result in the formation of compounds $Mn_2\{[(C_7H_5N_2)CH_2]_2NCH_2PO_3\}_2(H_2O)_2\cdot 2H_2O$, $Cd_2\{[(C_7H_5N_2)CH_2]_2NCH_2PO_3\}_2\cdot H_2O$, $Fe_2\{[(C_7H_5N_2)CH_2]_2NCH_2PO_3\}_2\cdot 2H_2O$, $Cu^I_2\{[(C_7H_5N_2)CH_2]_2NCH_2P(OH)O_2\}_2$[27], Ni_2(bbimp)$_2$ (4, 4′-bipy)$(H_2O)_2\cdot 2H_2O$, and [Ni_2(bbimp)$_2$ $(H_2O)_2$] [Ni (bbimp) $(H_2O)_2]_2\cdot 4H_2O$ [28]. The reactions of (benzimidazol-2-ylmethyl)iminobis(methylenephosph-onic acid) ($(C_7H_5N_2)CH_2N(CH_2PO_3H_2)_2$) with metal salts lead to five isomorphous compounds M $\{(C_7H_5N_2)CH_2N(CH_2PO_3H)_2\}$ (M=Mn, Fe, Co, Cu, Cd)[29]. In this article, we firstly report a new benzimidazole ligands: 2-(benzoimidazol-2-yl)phenylphosphonic acid ($C_7H_5N_2C_6H_4PO_3H_2$, 2-bppH$_3$), where a benzimidazole group is incorporated into the phenylphosphonic acid. Two new metal phosphonates based on this ligand, namely $[Mn(2\text{-}bppH_2)_2(H_2O)]_n$ (**1**) and $[Cu(2\text{-}bppH_2)_2]\cdot x CH_3OH$ (**2**) are obtained by hydro (solvo)-thermal methods. Compound **1** exhibits a one-dimensional chain structure, while compound **2** shows a discrete mononuclear structure. The magnetic and fluorescent properties of **1** are investigated.

1 Experimental

1.1 Materials and methods

The 2-(benzimidazol-2-yl)phenylphosphonic acid was prepared by a route beginning with ethyl 2-bromobenzoate[30]. All the other starting materials were of reagent grade quality and were obtained from commercial sources without further purification. The elemental analyses were performed with a PE 240C elemental analyzer. The infrared spectra were recorded on a VECTOR 22 spectrometer with pressed KBr pellets. Thermal analyses were performed with a METTLER TOLEDO TGA/DSC 1 instrument in the range of 30~800 ℃ under a nitrogen flow at a heating rate of 10 ℃·min^{-1}. Powder X-ray diffraction (XRD) data were collected on a Bruker D8 ADVANCE X-ray powder diffractometer (Cu $K\alpha$). The magnetic susceptibility data were obtained on polycrystalline samples using a Quantum Design MPMS-XL7 SQUID magnetometer. The data were corrected for diamagnetic contributions of both the sample holder and the compound obtained from Pascal′s constants[31].

1.2 Synthesis of $[Mn(2\text{-}bppH_2)_2(H_2O)]_n$ (1)

A mixture of 2-bppH$_3$ (0.10 mmol, 0.0274 g) and $MnSO_4\cdot H_2O$ (0.05 mmol, 0.008 5 g) in 6 mL H_2O (pH =6.20) was kept in a Teflon-lined autoclave at 140 ℃ for 24 h. After the mixture was cooled to room temperature, light pink blocky crystals were obtained as a monophasic material which is confirmed by the powder X-ray diffraction. Yield: 23 mg (74.4%, based on Mn). Anal. Found (Calcd.) for $C_{26}H_{22}MnN_4O_7P_2$ (%): C, 50.46 (50.37); H, 3.40 (3.55); N, 9.06 (9.04). IR (KBr, cm^{-1}): 3 632 (w), 3 197(br, w), 3 098(w), 3057 (w), 2 362(br, w) 1 843(w), 1 619(m), 1 559(m), 1 453 (m), 1 386(w), 1 318(w), 1 274(w), 1 228(w), 1 166(s), 1 149(s), 1 140(s), 1 113(s), 1 074(s), 1 051(s), 1 035 (s), 1 005(m), 967(s), 871(m), 815(m), 774(m), 748(s), 652(w), 618(m), 576(s), 568(s), 538(m), 514(m), 493 (m), 500 (w), 430 (w). Thermal analysis shows that compound **1** experiences the first step of weight loss below 138 ℃. The observed weight loss (2.8%) corresponds to the removal of one coordinated water molecule (Calcd. 2.9%). Above 346 ℃, the weight loss is due to the decomposition of the organic group.

1.3 Synthesis of $Cu(2\text{-}bppH_2)_2\cdot xCH_3OH$ (2)

A mixture of 2-bppH$_3$ (0.10 mmol, 0.0274 g) and $CuSO_4\cdot 5H_2O$ (0.10 mmol, 0.024 9 g) in 6 mL methanol was kept in a Teflon-lined autoclave at 70 ℃ for 24 h. After the mixture was cooled to room temperature, blue blocky crystals mixed with very small amount of unidentified green blocky crystals. The blue crystals, **2**, were picked out by hand. Yield: 13 mg (18.4%, based on Cu). Anal. Found (Calcd.) for $C_{26}H_{20}CuN_4O_6P_2\cdot CH_3OH$ (%): C, 51.01 (50.46); H,

3.48 (3.73); N, 9.07 (8.72). IR (KBr, cm^{-1}): 3 629 (w), 3 410 (w), 3 177~2 642 (br, w), 1 626(w), 1 596(w), 1 567 (w), 1 541 (w), 1 439 (s), 1 420 (s), 1 322 (w), 1 285(m), 1 196 (w), 1 147(s), 1 083 (s), 1 057 (s), 990 (m), 910 (s), 820 (w), 765 (m), 746 (s), 731 (m), 663 (w), 594 (s), 562 (w), 535 (m), 481 (w). Thermal analysis of the freshly prepared sample of **2** shows a two-step weight loss below 178 ℃ (Total 14.2%), in agreement with the removal of three methanol molecules (Calcd. 13.6%).

The lattice methanol is not stable, and can be released in air at room temperature. TG analysis of the sample placed in air for one week shows a single-step weight loss of 4.8% below 122 ℃, corresponding to the removal of 1.0 CH_3OH (Calcd. 4.8%). Above 325 ℃, the weight loss is due to the decomposition of the organic group.

1.4 Crystal structure determination

Single crystals of dimensions 0.3 mm×0.3 mm×0.2 mm for **1** and 0.3 mm×0.2 mm×0.2 mm for **2** were selected for diffraction data collection at 298 K on a Bruker SMART APEX CCD diffractometer equipped with graphite-monochromatized Mo $K\alpha$ (λ=0.071 073 nm) radiation. A hemisphere of data was collected in the θ range 1.76°~25.00° for **1** and 1.70°~25.00° for **2** using a narrow-frame method with scan widths of 0.30° in ω and an exposure time of 8 s per frame for **1** and 10 s for **2**. Numbers of measured and observed reflections ($I>2\sigma(I)$) are 6 376 and 2 309 (R_{int}=0.086 5) for **1** and 7 908 and 5 458 (R_{int}=0.042 1) for **2**, respectively.

The data were integrated using the Siemens SAINT program[32], with the intensities corrected for Lorentz factor, polarization, air absorption, and absorption due to variation in the path length through the detector faceplate. Multi-scan absorption corrections were applied. The structures were solved by direct methods, and were refined on F^2 by full matrix least squares using SHELXTL[33]. All the non-hydrogen atoms were refined anisotropically. All H atoms were added geometrically and refined isotropically. Crystallographic and refinement details are listed in Table 1. Selected bond lengths and angles are given in Tables 2.

CCDC: 913645, **1**; 913643, **2**.

Table 1 Crystallographic data for 1 and 2

Compound	**1**	**2**
Empirical formula	$C_{26}H_{22}MnN_4O_7P_2$	$C_{29}H_{32}CuN_4O_9P_2$
Formula weight	619.36	706.07
Crystal system	Monoclinic	Triclinic
Space group	$C2/c$	$P\bar{1}$
a / nm	1.581 3(4)	0.838 28(12)
b / nm	1.712 1(4)	1.224 19(18)
c / nm	0.982 9(2)	1.591 2(2)
β / (°)	98.770(4)	81.758(3)
V / nm^3	2.630 0(11)	1.579 0(4)
Z	4	2
D_c / (g·cm^{-3})	1.562	1.485
F(000)	1 264	730
R_{int}	0.086 5	0.042 1
Goodness-of-fit on F^2	1.005	0.991
R_1, wR_2 ($I>2\sigma(I)$)	0.040 1 / 0.091 0	0.053 8 / 0.097 3
R_1, wR_2 (All data)	0.055 8 / 0.100 7	0.073 5 / 0.104 5
$(\Delta\rho)_{max}$, $(\Delta\rho)_{min}$ / (e·nm^{-3})	460 / −903	557 / −363

$R_1=\Sigma||F_o|-|F_c||/\Sigma|F_o|$, $wR_2=[\Sigma w(F_o^2-F_c^2)^2/\Sigma w(F_o^2)^2]^{1/2}$

Table 2 Bond lengths (nm) and angles (°) for 1 and 2

1					
Mn1-O2i	0.20780(17)	P1-C12	0.1832(3)	O3iii-Mn1-O1W	85.43(15)
Mn1-O2ii	0.20780(17)	O2i-Mn1-O2ii	103.37(11)	O3-Mn1-O1W	81.51(15)
Mn1-O3iii	0.21139(17)	O2i-Mn1-O3iii	90.14(7)	O2i-Mn1-O1Wiii	114.78(12)
Mn1-O3	0.21140(17)	O2ii-Mn1-O3iii	98.20(7)	O2ii-Mn1-O1Wiii	141.84(12)
Mn1-O1W	0.2161(4)	O2i-Mn1-O3	98.20(7)	O3iii-Mn1-O1Wiii	81.50(15)
Mn1-O1Wiii	0.2161(4)	O2ii-Mn1-O3	90.14(7)	O3-Mn1-O1Wiii	85.43(15)
P1-O3	0.14986(17)	O3iii-Mn1-O3	166.57(9)	O1W-Mn1-O1Wiii	27.1(2)
P1-O1	0.15179(17)	O2i-Mn1-O1W	141.84(12)	P1-O2-Mn1i	142.35(11)
P1-O2	0.15235(17)	O2ii-Mn1-O1W	114.78(12)	P1-O3-Mn1	135.93(11)
2					
Cu1-O5	0.1901(2)	P1-O3	0.1566(2)	C7-N1-Cu1	125.0(3)
Cu1-O1	0.1911(2)	P1-C1	0.1809(4)	C13-N1-Cu1	128.1(3)
Cu1-N3	0.1971(3)	P2-O6	0.1492(3)	C20-N3-Cu1	129.5(3)
Cu1-N1	0.1990(3)	P2-O5	0.1501(3)	C26-N3-Cu1	123.3(3)
P1-O2	0.1489(2)	P2-O4	0.1564(3)	P1-O1-Cu1	132.22(15)

Symmetry transformations used to generate equivalent atoms: 1: (i) $-x$, $-y+1$, $-z+1$; (ii) x, $-y+1$, $z+1/2$; (iii) $-x$, y, $-z+3/2$

2 Results and discussion

2.1 Description of the structures

Compound **1** crystallizes in space group *C*2/*c*. The asymmetric unit contains 0.5 Mn, one 2-bppH$_2^-$ and 0.5 H$_2$O (Fig.1). The Mn atom locates on a mirror plane, with a distorted trigonal bipyramidal environment. Three equatorial bonding sites are occupied by two phosphonate oxygen atoms (O2i, O2ii) from two equivalent 2-bppH$_2^-$ ligands and one water oxygen atom (O1W). The water molecule is disordered over two sites, each with the occupancy of 50%. The sum of the equatorial O-Mn-O angles is 360°. The axial sites are filled with two phosphonate oxygen atoms (O3, O3iii) from two equivalent 2-bppH$_2^-$ ligand. The Mn-O bond lengths are in the range of 0.195 6 (3)~0.240 7 (5) nm (Table 2). Each 2-bppH$_2^-$ ligand serves as a bidentate ligand, bridging the equivalent Mn atoms through its two phosphonate oxygen donors (O2, O3) to form an infinite chain running along the *c* axis (Fig.2). The benzimidazole group, with N1 atom protonated, is not involved in the coordination with metal ions.

Hydrogen bond interactions are found among the imidazole nitrogen atoms (N1, N2), the phosphonate oxygen atoms (O1, O2) and coordination water oxygen

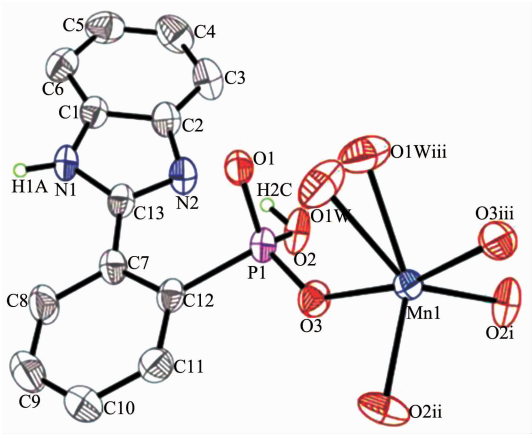

All H atoms except H1A are omitted for clarity. Symmetry codes: (i) $-x$, $-y+1$, $-z+1$; (ii) x, $-y+1$, $z+1/2$; (iii) $-x$, y, $-z+3/2$

Fig.1 Building unit of **1** in ORTEP view with 50% thermal ellipsoids

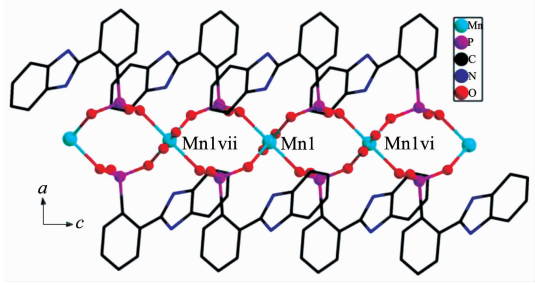

All H atoms are omitted for clarity. Symmetry codes: (vi) $-x$, $-y+1$, $-z+2$; (vii) $-x$, $-y+1$, $-z+1$

Fig.2 A fragment of chain in compound **1**

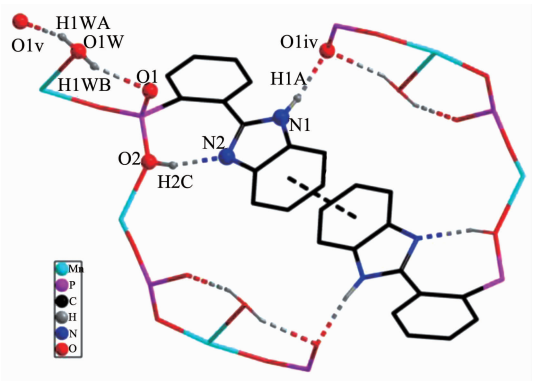

Symmetry codes: (iv) $-x+1/2$, $-y+1/2$, $-z+1$; (v) $-x$, y, $-z+3/2$

Fig.3　Inter- and intra-chain hydrogen bond and π-π interactions in compound **1**

atom (O1W) from intra- and inter- chains (Fig.3). The N1 ··· O1iv, O2 ··· N2, and O1W ··· O1v distances are 0.2629 (5), 0.2583 (0) and 0.2662 (4) nm, respectively (symmetry codes: iv: $-x+1/2$, $-y+1/2$, $-z+1$; v: $-x$, y, $-z+3/2$). There are π-π interactions between the benzimidazole rings from the adjacent chains. The average centroid-centroid distance between the two phenyl rings of the benzimidazole groups is 0.364 3(3) nm (Fig.3)[34]. Therefore, a three-dimensional network structure is built up through weak interactions (Fig.4).

Compound **2** crystallizes in space group $P\bar{1}$. The asymmetric unit contains one Cu, two 2-bppH$_2^-$ and three lattice CH$_3$OH molecules. It shows discrete mononuclear structure (Fig.5). The Cu atom is four-coordinated with a distorted quadrilateral geometry, with the binding sites provided by two phosphonate oxygen atoms (O1, O5) and two nitrogen atoms (N1, N3). The Cu-O and Cu-N bond lengths are in the range of 0.190 1(2)~0.191 1(2) nm and 0.197 1(3)~0.199 0(3) nm, respectively. Each 2-bppH$_2^-$ ligand acts as a bidentate chelating ligand using one phosphonate oxygen and one nitrogen atoms. The remaining two phosphonate oxygen atoms are either protonated or pendent. The remaining benzimidazole nitrogen (N2, N4) atoms are also protonated. The π-π interactions are observed between the 2-bppH$_2^-$ ligands from neighboring mononuclear units (Fig.6). Extensive hydrogen bond interactions are found between the imidazole nitrogen atom (N2, N4), the phosphonate oxygen atom (O2, O3, O4 and O6) and methanol oxygen

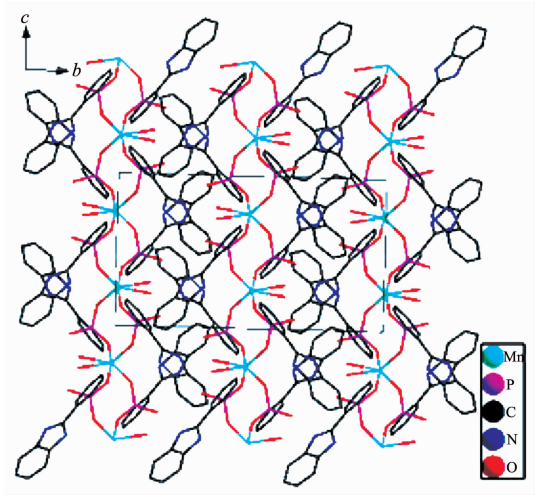

All H atoms are omitted for clarity

Fig.4　Packing diagram of compound **1** projected along a axis

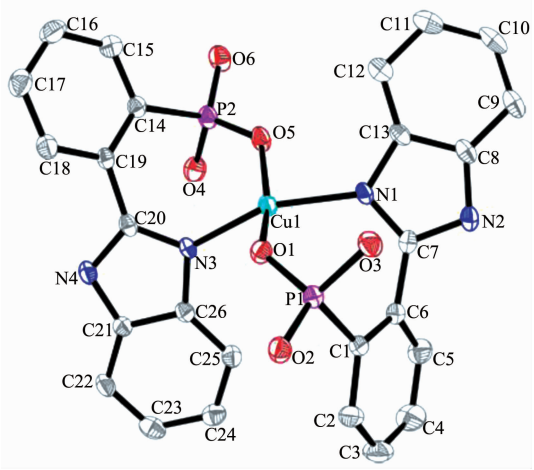

All H atoms except those attached to imidazole and phosphonate groups are omitted for clarity

Fig.5　Mononuclear structure of **2** in ORTEP view with 50% thermal ellipsoids

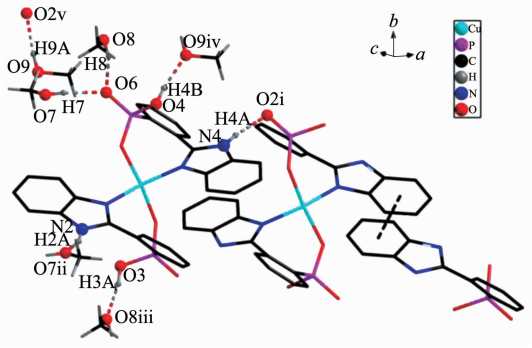

Symmetry codes: (i) $-x+2$, $-y+1$, $-z+1$; (ii) $-x+1$, $-y+1$, $-z+2$; (iii) x, $y-1$, z; (iv) $x+1$, y, z; (v) $x-1$, $y+1$, z

Fig.6　Hydrogen bond and π-π interactions in compound **2**

Table 3 Hydrogen bond lengths and angles for 2

D-H···A	*d*(D-H) / nm	*d*(H···A) / nm	*d*(D···A) / nm	∠DHA / (°)
N4-H4A···O2i	0.086 0	0.195 2	0.280 6	171.88
N2-H2A···O7ii	0.086 0	0.196 0	0.277 4	157.40
O3-H3A···O8iii	0.082 0	0.171 7	0.252 4	167.27
O4-H4B···O9iv	0.082 0	0.174 9	0.255 1	165.61
O7-H7···O6	0.082 0	0.190 6	0.272 1	172.39
O8-H8···O6	0.082 0	0.185 6	0.263 9	159.25
O9-H9A···O2v	0.082 0	0.182 8	0.264 5	173.87

Symmetry codes: (i) $-x+2, -y+1, -z+1$; (ii) $-x+1, -y+1, -z+2$; (iii) $x, y-1, z$; (iv) $x+1, y, z$; (v) $x-1, y+1, z$

atom (O7, O8 and O9) (Table 3). Therefore, a three-dimensional supramolecular network structure is constructed.

2.2 Magnetic property

The magnetic property of compound **1** was investigated in the temperature range of 1.8~300 K. The effective magnetic moment per Mn at 300 K is 5.89μ_B, close to the theoretical value (5.92μ_B) for a single Mn^{II} with spin S=5/2 and g=2. The continuous decrease of $\chi_M T$ upon cooling suggests a dominant antiferromagnetic exchange coupling between the Mn^{II} centers. Since structure **1** is one-dimensional and the Mn^{II} ions are linked purely through O-P-O units, the susceptibility data can be analyzed by Fishers expression for a uniform chain based on the Heisenberg Hamiltonian $H=-J\Sigma S_{Ai}\cdot S_{Ai+1}$, with the classical spins scaled to a real quantum spin S=5/2 (Equation **1**)[31]:

$$\chi_M = \frac{Ng^2\beta^2 S(S+1)}{3kT}\frac{1+u}{1-u}$$

$$u = \coth\left[\frac{JS(S+1)}{kT}\right] - \frac{kT}{JS(S+1)} \qquad (\mathbf{1})$$

where J is the coupling constant, N, g, β and k have their usual meanings. A good fit, shown as the solid line in Fig.7, gives the parameters g=2.01 and J=−0.08 cm^{-1}. The field dependent magnetization at 1.8 K reveals that the magnetization at 70 kOe is 4.8$N\beta$, close to the saturation value of 5.0$N\beta$ for Mn (S=5/2, g=2.0) (inset of Fig.7).

2.3 Fluorescent property

The fluorescent properties of free 2-bppH$_3$ ligand and compound **1** in solid state at room temperature are depicted in Fig.8. Clearly, excitation at 417 nm leads to fluorescent emission bands at ca. 531 and 585 nm for **1**,

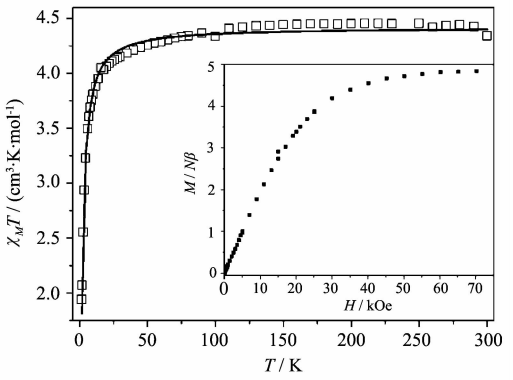

Insert: plot of M vs. H for **1** at 1.8 K

Fig.7 χ_MT vs. T plot for **1**

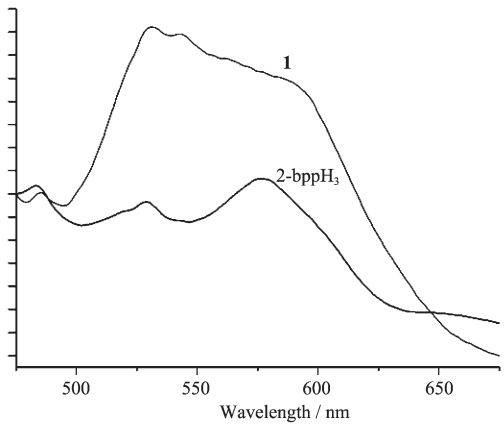

Fig.8 Emission spectra of 2-bppH$_3$ and compound **1** in solid state at room temperature

which are similar to those for free 2-bppH$_3$ ligand (ca. 529 and 576 nm). Thus the broad emission bands can be assigned to the intra-ligand $^1(\pi\text{-}\pi^*)$ fluorescence emission of 2-bppH$_3$ [33-35]. The greater fluorescent intensity of the ligand upon coordination may presumably be due to the increase in conformational rigidity which reduces the loss of energy via

radiationless decay of the intra-ligand emission excited state.

3 Conclusions

By using 2-(benzoimidazol-2-yl)phenylphosphonic acid, we obtained two compounds with the formula [Mn(2-bppH$_2$)$_2$(H$_2$O)]$_n$ (**1**) and [Cu(2-bppH$_2$)$_2$]·xCH$_3$OH (**2**). Compound **1** exhibits one-dimensional chain structure, while compound **2** shows a discrete mononuclear structure. The benzimidazole rings are involved in both hydrogen bonds and π-π interactions. Magnetic studies of **1** reveal that a weak antiferromagnetic interaction is propagated between the manganese centers via O-P-O bridge. Further work is in progress to explore new materials with other structures based on the same phosphonate ligand.

Acknowledgement

This work is supported by the NSF of Jiangsu Province (No. BK2009009).

References:

[1] Maillet C, Janvier P, Pipelier M, et al. *Chem. Mater.*, **2001**, **13**:2879-2884

[2] Hu A, Ngo H L, Lin W B. *Angew. Chem. Int. Ed.*, **2003**,**42** (48):6000-6003

[3] Ayyappan P, Evans O R, Cui Y, et al. *Inorg. Chem.*, **2002**, **41**:4978-4980

[4] Kong D Y, Li Y, Ross J H, et al. *Chem. Commun.*, **2003**, 1720-1721

[5] Yin P, Gao S, Wang Z M, et al. *Inorg. Chem*., **2005**,**44**:2761-2765

[6] Maheswaran S, Chastanet G, Teat S J, et al. *Angew. Chem. Int. Ed.*, **2005**,**44**:5044-5048

[7] Langley S, Helliwell M, Raftery J, et al. *Chem. Commun.*, **2004**,142-143

[8] Nonglaton G, Benitez I O, Guisle I, et al. *J. Am. Chem. Soc*., **2004**,**126**:1497-1502

[9] Fredoueil F, Massiot D, Janvier P, et al. *Inorg. Chem*., **1999**,**38**:1831~1833

[10]Zhu J, Bu X H, Feng P Y, et al. *J. Am. Chem. Soc.*, **2000**, **122**:11563-11564.

[11]Wang P F, Duan Y, Clemente-Juan J M, et al. *Chem. Eur. J*., **2011**,**17**:3579-3583

[12]Guo L R, Bao S S, Zheng L M. *Solid State Sci*., **2009**,**11**: 310-314

[13]Yang T H, Liao Y, Zheng L M, et al. *Chem. Commun*., **2009**:3023-3025

[14]Guo L R, Bao S S, Li Y Z, et al. *Chem. Commun.*, **2009**: 2893-2895

[15]Bao S S, Chen G S, Wang Y, et al. *Inorg. Chem*., **2006**,**45**: 1124-1129

[16]Clearfield A, Poojary D M, Zhang B L, et al. *Chem. Mater*., **2000**,**12**:2745-2752

[17]Moulton B, Zaworotko M J. *Chem. Rev*., **2001**,**101**:1629-1658

[18]Guckian K M, Morales J C, Kool E T. *J. Org. Chem*., **1998**,**63**:9652-9656

[19]Morales J C, Kool E T. *Nat. Struct. Bio.*, **1998**,**5**:950-954

[20]Tamm I, Folkers K, Shunk C H. *J. Bacter*., **1956**,**72**:59-64

[21]Morales J C, Kool E T. *J. Am. Chem. Soc.*, **1999**,**121**:2323-2324

[22]Skalitzky D J, Marakovits J T, Maegley K A, et al. *J. Med. Chem.*, **2003**,**46**:210-213

[23]Murray M, Ryan A J, Little P J. *J. Med. Chem.*, **1982**,**25**: 887-892

[24]Trivulzio S, Colombo R, Rossoni G, et al. *Pharmacol. Res. Commun.*, **1988**,**20**:975-982

[25]Ersan S, Nacak S, Noyanalpan N, et al. *Arzneimittel-Forsch.*, **1997**,**47**:834-836

[26]Hauel N H, Nar H, Priepke H, et al. *J. Med. Chem.*, **2002**, **45**:1757-1766

[27]Cao D K, Xiao J, Tong J W, et al. *Inorg. Chem.*, **2007**,**46**: 428-436

[28]CAO Deng-Ke (曹登科), XIAO Jing (肖婧), LI Yi-Zhi (李一志), et al. *Chinese J. Inorg. Chem.* (*Wuji Huaxue Xuebao*), **2007**,**23**:1947-1953

[29]Cao D K, Xiao J, Li Y Z, et al. *Eur. J. Inorg. Chem.*, **2006**, 1830-1837

[30]Moedritz K, Irani R R. *J. Org. Chem.*, **1966**,**31**:1603-1607

[31]Kahn O. *Molecular Magnetism*. New York: VCH Publishers, **1993**.

[32]SAINT, *Program for Data Extraction and Reduction*, Siemens Analytical X-ray Instruments, Madison, WI, **1994-1996**

[33]*SHELXTL* (*version* 5.0), *Reference Manual*, Siemens Industrial Automation, Analytical Instruments, Madison, WI, **1995**.

[34]Janiak C. *J. Chem. Soc*., *Dalton Trans*., **2000**,3885-3896

[35]Dutta B, Bag P, Flörke U, et al. *Inorg. Chem.*, **2005**,**44**:147-157

[36]Banthia S, Samanta A. *J. Phys. Chem. B*, **2006**,**110**:6437-6440

[37]Chen W, Peng Q, Li Y D. *Cryst. Growth Des*., **2008**,**8**:564-567